Turbulence in wall-bounded flows

Sergio Pirozzoli Matteo Bernardini Paolo Orlandi

Dipartimento di Ingegneria Meccanica ed Aerospaziale
"Sapienza" Universita' di Roma

HPC methods for Computational Fluid Dynamics and Astrophysics
November 2-4 2016, Bologna

sergio.pirozzoli@uniroma1.it

Acknowledgments

- All simulations carried out using PRACE resources
  - PRACE 3rd call
  - PRACE 5th call
  - PRACE 7th call
  - PRACE 10th call
  - PRACE 12th call
- Thanks to CINECA staff!

Why wall turbulence?

- Flow over solid surfaces most often turbulent
- Turbulent flow $\rightsquigarrow$ large increase of drag and heat transfer as compared to laminar state
- Drag and heat transfer prediction critical for efficient design of aircraft, cars, pipelines, ...
- Practical impact: 1% drag reduction of A340 would result in fuel savings of about 100,000 Euros per aircraft per year
- Robust physical insight definitely needed

Wall turbulence: how it looks like

Side view of turbulent flow over smooth horizontal surface ($Re_\tau \approx 4000$)

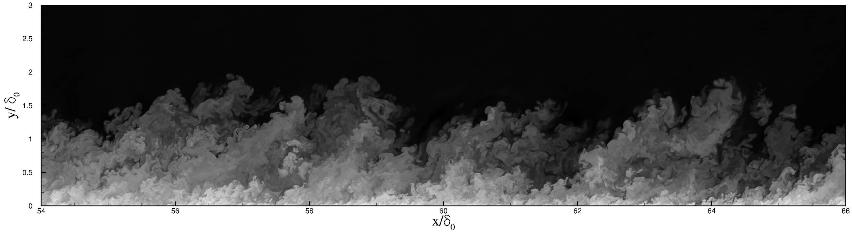

Wall-parallel view of turbulent flow over smooth horizontal surface ($Re_\tau \approx 4000$)

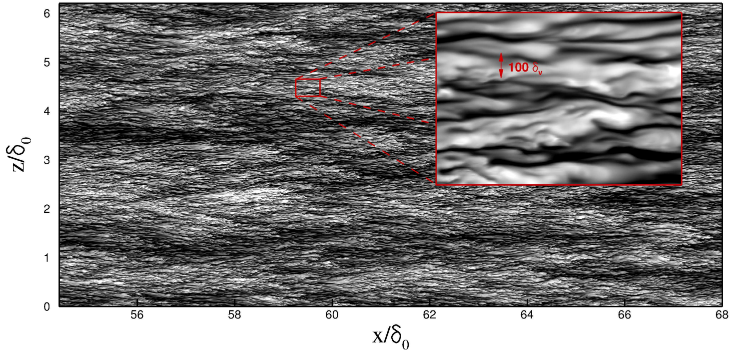

Wall turbulence: a cartoon

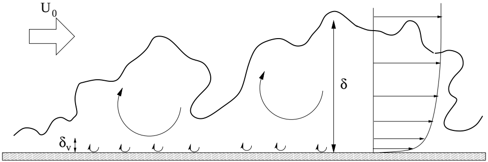

- Two velocity scales
  1. U_0 (outer scale)
  2. $u_\tau = (\tau_w/\rho)^{1/2}$ (inner scale)
- Two length scales
  1. δ (outer scale)
  2. $\delta_v = \nu/u_\tau$ (inner scale)
- Ratio of outer to inner length scales is an important parameter

$$Re_\tau = \delta u_\tau/\nu = \delta/\delta_v$$

Wall turbulence: what we know

- (Approximately) universal near-wall behavior in inner scales, i.e.

$$u^+ := \overline{u}/u_\tau = f(y^+), \quad y^+ := y/\delta_v$$

- Logarithmic meso-layer of mean velocity (Prandtl 25)

$$u^+ = 1/k \log y^+ + C, \quad k = 0.41, C \approx 5$$

- Logarithmic layer of wall-parallel velocity variances (Townsend 76)

$$\overline{u'^2}/u_\tau^2 = -A \log y/\delta + B$$

- The latter implies that peak velocity variances grow as $\log Re_\tau$

Wall turbulence: what we don't know

- High $Re_\tau \rightsquigarrow$ outer eddies become more energetic
- Inner-outer layer interactions become more important
- Corrections to classical representation

$$u^+ = f(y^+, Re_\tau)$$

- Asymptotic limit as $Re_\tau \to \infty$?
- Subject of several recent reviews (Jimenez 2013, Smits et al. 2011, Marusic et al. 2010)

Why use supercomputers?

- Experiments limited in near-wall resolution, and difficulty to get 'clean' data (e.g. derivatives of flow statistics)
- Revert to Direct Numerical Simulation (DNS), i.e. solve full Navier-Stokes equations in 3D unsteady version by resolving all scales of motion
- However, DNS of wall turbulence hampered by stringent computational requirements
- As $\Delta \sim \delta_v$, simulating flows at high Re_τ requires about $(\delta/\Delta)^3 = Re_\tau^3$ points (in fact, $N_{\text{pts}} \sim Re_\tau^{11/4}$)
- Some effects (e.g. logarithmic scaling) only manifest themselves as $Re_\tau \sim 10^3 - 10^4 \rightsquigarrow O(10^9 - 10^{12})$ points are required

State-of-the-art

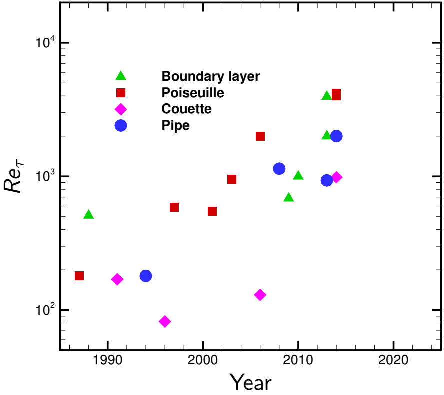

Projection

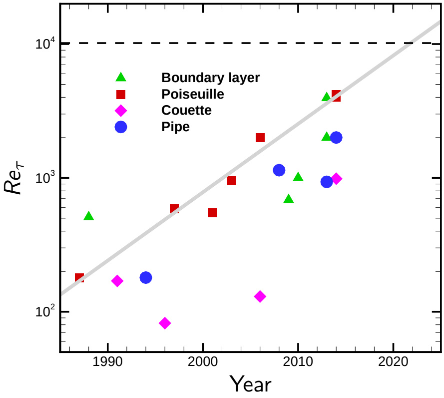

- $Re_\tau \approx 10^4$ likely to yield 'asymptotic' wall turbulence (Jimenez 2012)

Outline

- DNS of incompressible wall-bounded flows ($M = 0$)
  - Poiseuille flow up to $Re_\tau \approx 4000$
  - Couette flow up to $Re_\tau \approx 1000$
  - Passive scalars in Poiseuille flow
  - Channel flow with unstable stratification
- DNS of compressible wall-bounded flows: see next talk

Navier-Stokes-Boussinesq model

$$\frac{\partial u_j}{\partial x_j} = 0, \quad \frac{\partial u_i}{\partial t} + \frac{\partial u_i u_j}{\partial x_j} = -\frac{\partial p}{\partial x_i} + \beta g \theta \delta_{i2} + \Pi \delta_{i1} + \nu \frac{\partial^2 u_i}{\partial x_j \partial x_j}$$

$$\frac{\partial \theta}{\partial t} + \frac{\partial \theta u_j}{\partial x_j} = \alpha \frac{\partial^2 \theta}{\partial x_j \partial x_j}$$

Controlling parameters

- Convection: bulk Reynolds number $Re_b = 2hu_b/\nu$
- Buoyancy: bulk Rayleigh number $Ra = \beta g \Delta\theta (2h)^3/(\alpha\nu)$
- Buoyancy/convection: bulk Richardson number $Ri_b = Ra/Re_b^2 = 2\beta g \Delta\theta h/u_b^2$
- $Pr = \nu/\alpha \equiv 1$

Numerical method

Orlandi 2000

- Projection method with direct Poisson solver based on Fourier expansions (Kim & Moin 87)
- Second-order approximation of space derivatives on staggered mesh (Harlow & Welch 65)
- Discrete conservation of total kinetic energy and scalar variance
- Implicit treatment of wall-normal viscous terms
- Third-order low-storage Runge-Kutta time stepping by A. Wray
- Pencil decomposition for efficient parallel implementation

Numerical discretization

- Incompressible NS equations

$$\frac{\partial u_j}{\partial x_j} = 0, \quad \frac{\partial u_i}{\partial t} + \frac{\partial u_i u_j}{\partial x_j} = -\frac{\partial p}{\partial x_i} + \nu \frac{\partial^2 u_i}{\partial x_j \partial x_j}$$

- Projection method to satisfy divergence-free constraint
- Semi-implicit discretization in time

$$\frac{v^* - v^n}{\Delta t} = N^{n+1/2} + \frac{1}{2}\left(L(v^*) + L(v^n)\right) - Gp^n \quad (\mathbf{1})$$

- In general, v^* is not divergence-free
- For that purpose, a correction step is implemented

$$\frac{v^{n+1} - v^*}{\Delta t} = -G\varphi \quad (\mathbf{2})$$

with φ TBD

Numerical discretization

- Take discrete divergence of previous equations

$$G \cdot G\varphi = -\frac{G \cdot \left(v^{n+1} - v^*\right)}{\Delta t} = \frac{G \cdot v^*}{\Delta t}$$

- Discrete Poisson equation
- Relation between φ and pressure can be derived by combining steps (1) and (2)

$$p^{n+1} = p^n + \varphi + \frac{1}{2} L\varphi$$

- The latter relation is used to feed step (1)

Computational issues

- Inviscid 1D case

$$\frac{v_j^{n+1} - v_j^*}{\Delta t} = -D\varphi_j \rightsquigarrow D \cdot D\varphi = \frac{Dv^*}{\Delta t}$$

- Assume $D = C2$

$$\varphi_{j-2} - 2\varphi_j + \varphi_{j+2} = h\,\frac{v_{j+1}^* - v_{j-1}^*}{2\Delta t}$$

- The stencil $(j-2, j, j+2)$ only contains odd or even indices $\rightsquigarrow$ decoupling of discrete pressure field

Avoiding odd-even decoupling

- Staggered grid arrangement (MAC method, Harlow & Welch 65)

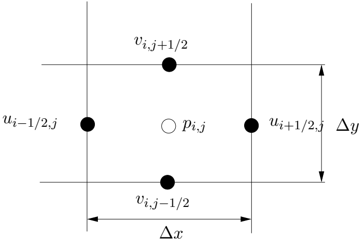

$$\left[\frac{\partial u^2}{\partial x}\right]_{i+1/2,j} = \frac{u^2_{i+1,j} - u^2_{i,j}}{\Delta x} + O(\Delta x^2)$$

$$\left[\frac{\partial uv}{\partial y}\right]_{i+1/2,j} = \frac{\left[(uv)_{i+1/2,j+1/2} - (uv)_{i+1/2,j-1/2}\right]}{\Delta y} + O(\Delta y^2)$$

$$\left[\frac{\partial^2 u^2}{\partial x^2}\right]_{i+1/2,j} = \frac{u_{i+3/2,j} - 2u_{i+1/2,j} + u_{i-1/2,j}}{\Delta x^2} + O(\Delta x^2)$$

$$\left[\frac{\partial p}{\partial x}\right]_{i+1/2,j} = \frac{p_{i+1,j} - p_{i,j}}{\Delta x} + O(\Delta x^2)$$

Avoiding odd-even decoupling

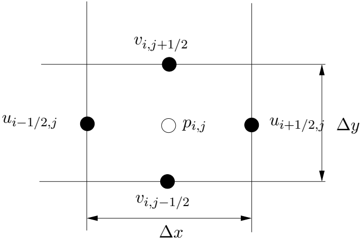

- Interpolations are needed

$$u_{i+1,j} = 0.5\left(u_{i+1/2,j} + u_{i+3/2,j}\right)$$

$$(uv)_{i+1/2,j+1/2} = \left[u_{i+1/2,j} + u_{i+1/2,j+1}\right] \cdot$$
$$\cdot \left[v_{i+1,j+1/2} + v_{i,j+1/2}\right] /4$$

- Connection with skew-symmetric form $\rightsquigarrow$ discrete energy conservation

$$\begin{aligned}
\left[\frac{\partial u^2}{\partial x}\right]_{i+1/2,j} &\approx \frac{\left(u_{i+1/2,j} + u_{i+3/2,j}\right)^2 - \left(u_{i-1/2,j} + u_{i+1/2,j}\right)^2}{4\Delta x} \\
&= \frac{u^2_{j+3/2} - u^2_{j-1/2}}{4\Delta x} + u_{i+1/2}\frac{u_{i+3/2,j} - u_{i-1/2,j}}{2\Delta x} \\
&\approx \frac{1}{2}\frac{\partial u^2}{\partial x} + u\frac{\partial u}{\partial x}
\end{aligned}$$

Solution of Poisson equation for φ

$$G \cdot G\varphi = G \cdot v^*/\Delta t$$

- In general requires iterative solvers $\rightsquigarrow$ impractical for DNS
- Direct solvers available in the presence of two periodic/symmetric directions (Kim & Moin 87)
- Fourier expansion in homogeneous directions (say x, z)

$$\varphi(x, y, z) = \sum_{\ell,m} \hat{\varphi}_{\ell,m}(y) e^{ik_\ell x} e^{ik_m z}$$

  $k_\ell = 2\pi\ell/L_x$, $k_m = 2\pi m/L_z$
- Set $f = G \cdot v^*/\Delta t$

$$-\hat{\varphi}_{\ell,m}\left(\tilde{k}_{x_2} + \tilde{k}_{z_2}\right) + D_{y2}\hat{\varphi}_{\ell,m} = \hat{f}_{\ell,m}$$

- $\tilde{k}_{x_2}$, $\tilde{k}_{z2}$ are MWN for the second space derivative, e.g. $\tilde{k}_{x_2} = 2(1 - \cos(k_\ell \Delta x))/\Delta x^2$, $\tilde{k}_{z_2} = 2(1 - \cos(k_m \Delta z))/\Delta z^2$
- Standard tridiagonal system in y direction must be solved $\forall \ell, m$

Accuracy

- Linear analysis not necessarily the 'ultimate word'
- Simple exercise: consider Burgers vortex model
- Representative for small-scale vortex tubes (Jimenez 93)

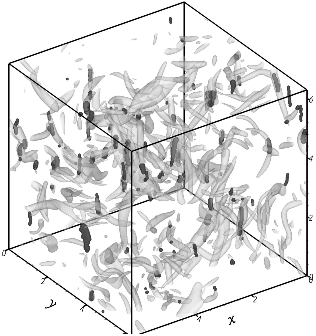

$$u_\theta(x) \sim \frac{1}{\xi}\left(1 - e^{-\xi^2}\right)$$

$\xi = x/r_b$, $r_b = 3.94\eta$

- We evaluate a single derivative as in MAC method

$$\frac{u_{j+3/2}^2 - u_{j-1/2}^2}{4\Delta x} + u_{i+1/2}\frac{u_{i+3/2,j} - u_{i-1/2,j}}{2\Delta x} \approx \frac{1}{2}\frac{\partial u^2}{\partial x} + u\frac{\partial u}{\partial x}$$

Error analysis

- L_2 error norm

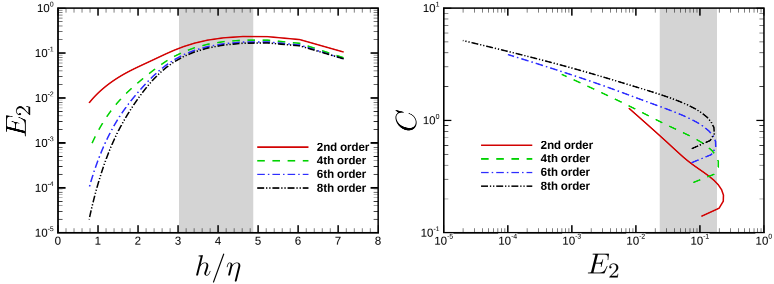

- Practical DNS of wall turbulence use typical grid spacings in the wall-parallel direction $\Delta x/\eta \gtrsim 5$, $\Delta z/\eta \gtrsim 3$
- FD formulas still far from reaching the asymptotic convergence limit
- The additional computational cost may not be justified
- MAC scheme successfully used for DNS of many wall-bounded flows

FD vs. spectral

- Plane channel at $Re_\tau = 2000$
- Lines: second-order finite differences (Bernardini et al. 14); symbols: pseudo-spectral method (Hoyas & Jimenez 06)

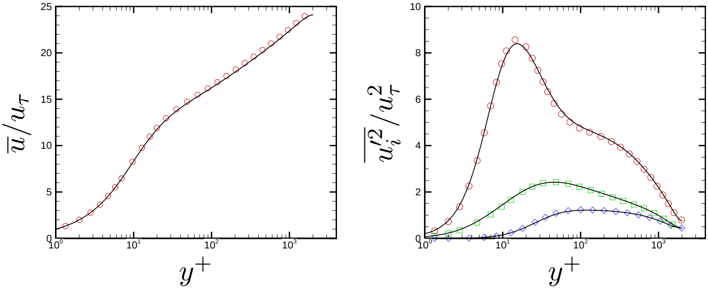

- Max difference about $< 2\%$ in turbulence intensity

Parallel implementation

Slab vs. pencil decomposition

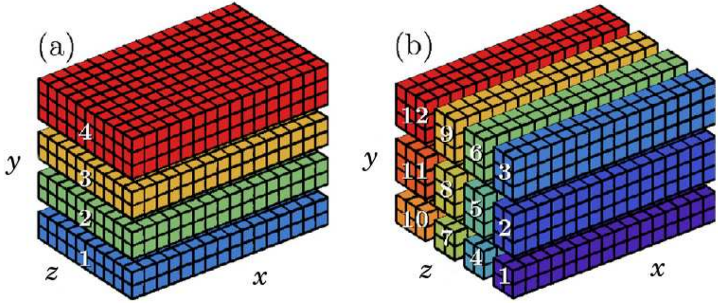

- Operations in $x - z$ plane can be carried out locally
- Operations in y (e.g. tridiagonal matrix inversion in Poisson solver) are global, requiring data transposition
- Main limitation: given N^3 mesh, max N processors can be used
- E.g. 10^9 points can be (inefficiently) handled on 1000 MPI processes
- Number of halo cells gets higher as $\#$ of cores increases

Parallel implementation

Pencil decomposition

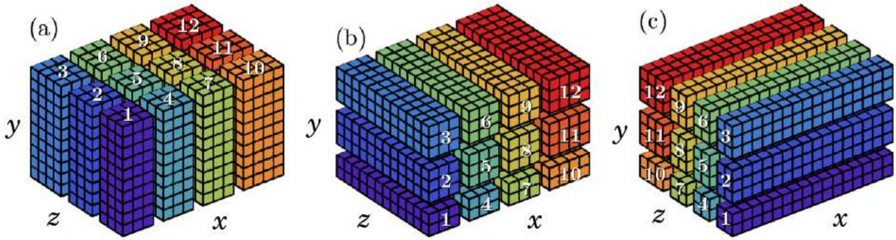

- The limit on the number of processes is now $N_p = N^2$
- Size of the halo cells on every core decreases with increasing # cores
- Example of work flow: solution of Poisson equation
    1. transpose (a)→(b), then take real FT in z
    2. transpose (b)→(c), then take complex FT in x
    3. transpose (c)→(a), then solve tridiagonal system in $y \rightsquigarrow$ Fourier coefficients
    4. Transpose (a)→(c), then take inverse FT in x
    5. Transpose (c)→(b), then take inverse FT in z to get physical solution
    6. Transpose (b)→(a) to have solution in original arrangement

Weak scaling

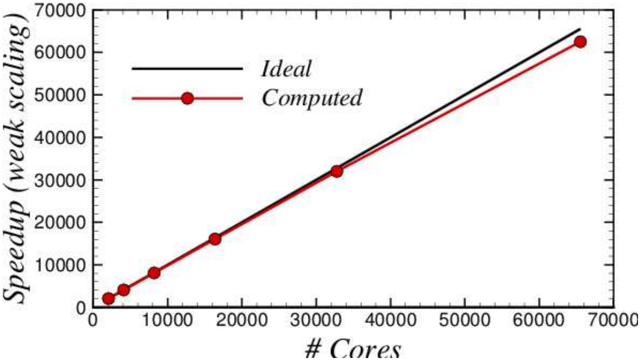

DNS setup

Flow case	Line style	Re_b	Re_τ	N_x	N_y	N_z	Δx^+	Δz^+	Tu_τ/h
CH1	Dashed	20063	546	1024	256	512	10.0	6.7	36.3
CH2	Dash-dot	39600	999	2048	384	1024	9.2	6.1	26.9
CH3	Dash-dot-dot	87067	2012	4096	768	2048	9.3	6.2	14.9
CH4	Solid	191333	4079	8192	1024	4096	9.4	6.2	8.54

- Computational box $L_x = 6\pi h$, $L_z = 2\pi h$

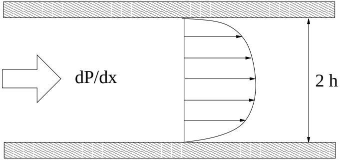

DNS at $Re_\tau = 4000$: contour lines of u'

low-speed and high-speed

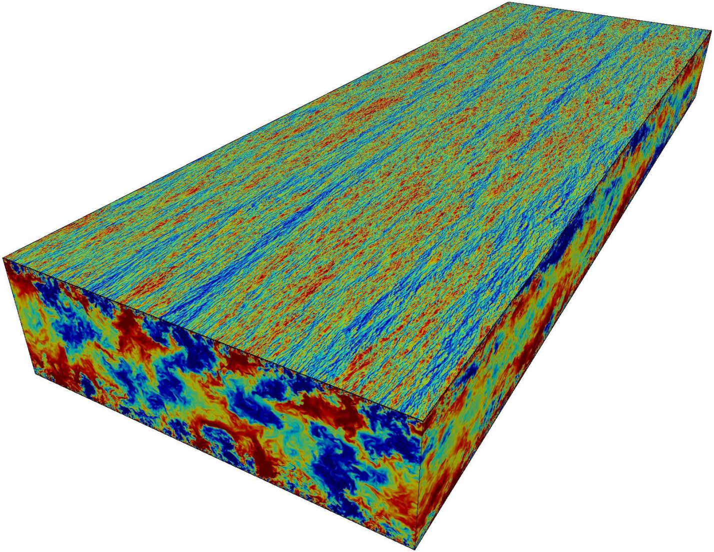

Mean velocity

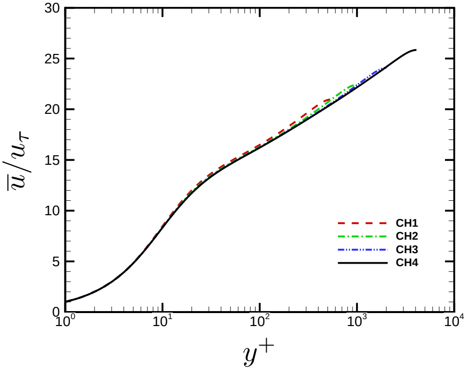

Mean velocity

Comparison with experiments

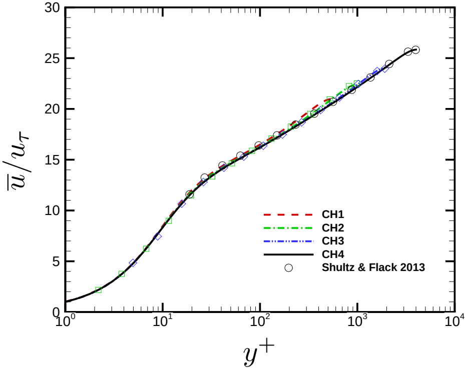

DNS of Poiseuille flow

Mean velocity

Overlap layer

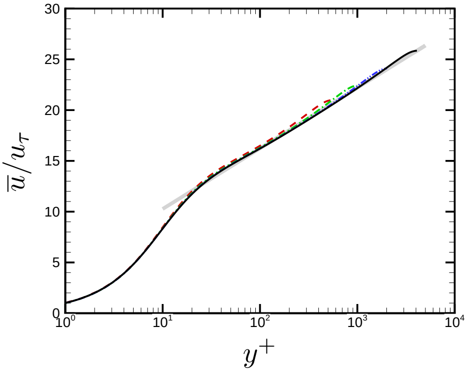

- Log-law fit $\quad u^+ = 4.30 + \log y^+ / 0.386$
- Recent estimates yield $k \approx 0.37, C = 3.7$ (Nagib PoF 2008)

Diagnostic function $\Xi = y^+ \, \mathrm{d}\overline{u}^+ / \mathrm{d}y^+$

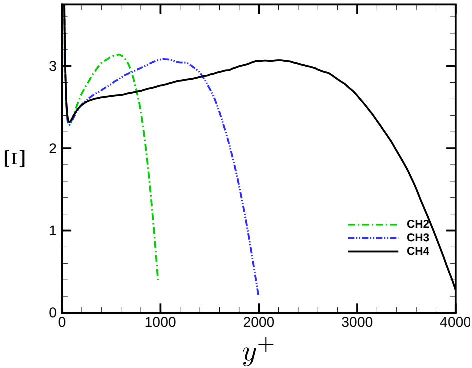

- No range with flat behavior

Diagnostic function $\Xi = y^+ \, \mathrm{d}\overline{u}^+/\mathrm{d}y^+$

Generalized log law

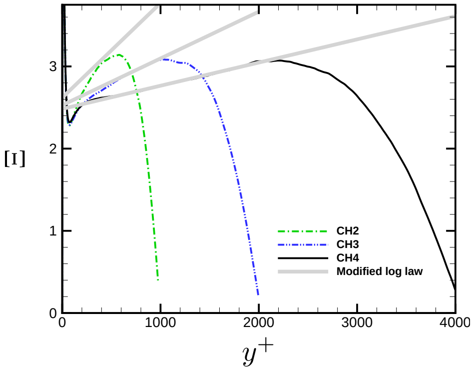

- Refined overlap arguments (Afzal 1976) suggest $\Xi = \dfrac{1}{k} + \alpha \dfrac{y}{h} + \dfrac{\beta}{Re_\tau}$
- We get $k = 0.41$, $\alpha = 1.15$, $\beta = 180$ (close to Jimenez & Moser 2007)

Velocity variances

Horizontal components

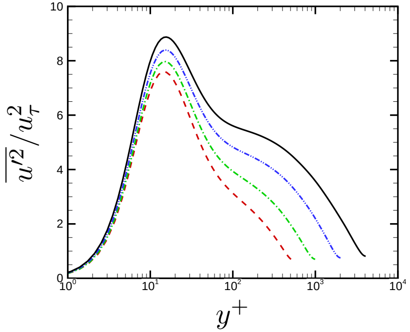

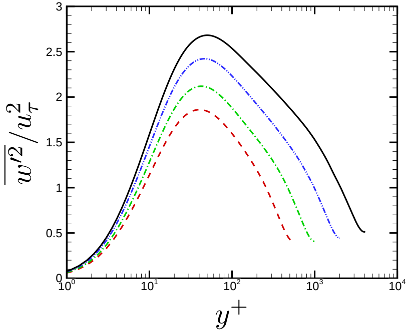

Velocity variances

Horizontal components

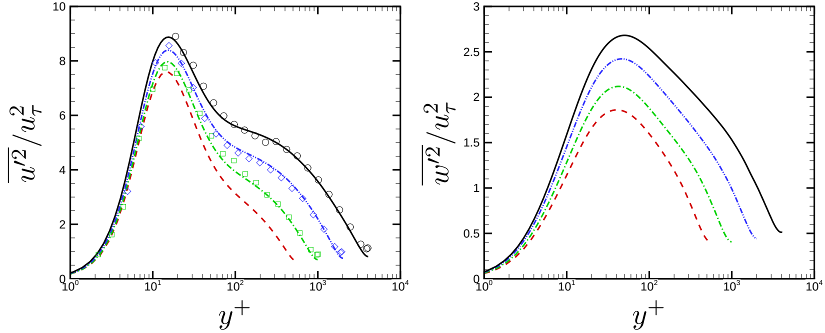

- Experiments by Shultz & Flack (2013)

Velocity variances

Horizontal components

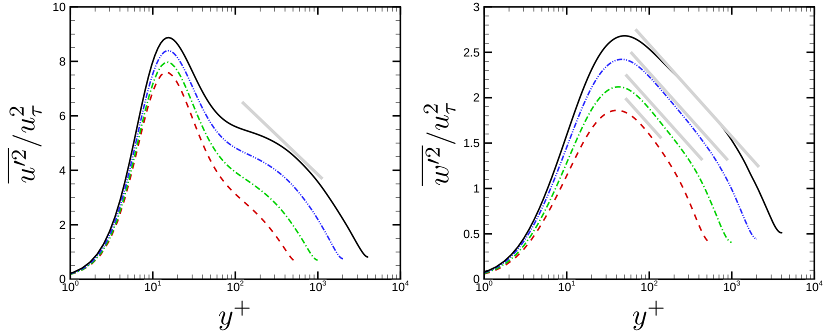

- Townsend attached-eddy hypothesis: $\overline{u_i'^2}/u_\tau^2 \approx B_i - A_i \log(y/h)$
- Typically quoted values $A_1 \approx 1.26$, $B_1 \approx 1.7$
- We find $A_3 \approx 0.44$, $B_3 \approx 0.95$

Reynolds stress peaks

Trend with Re_τ

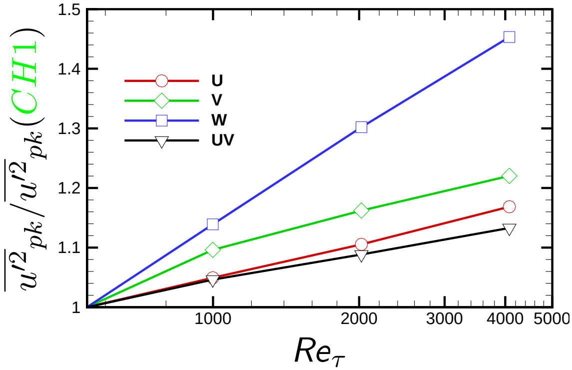

- Clear logarithmic growth of u and w
- Sub-logarithmic growth of v

Spectral densities (pre-multiplied)

u, inner scaling

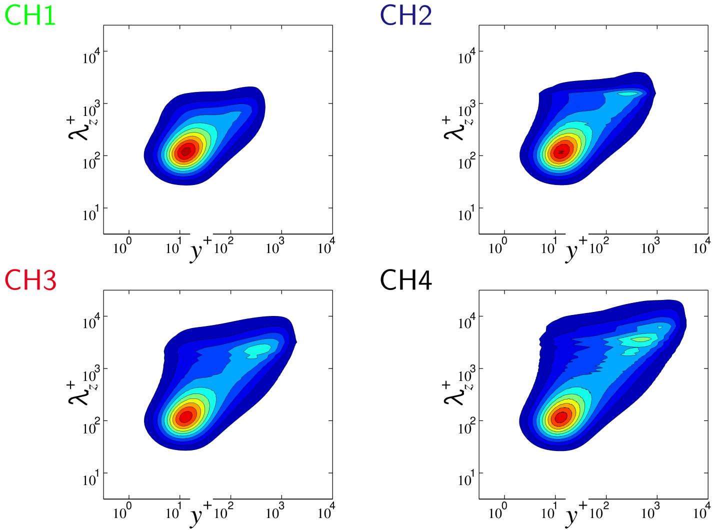

Production excess over dissipation

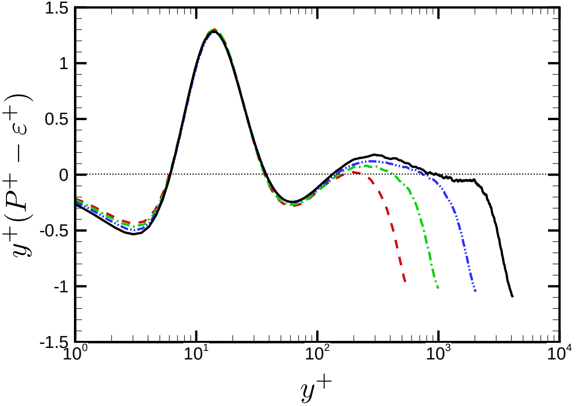

- Equilibrium hypothesis clearly violated at sufficiently high Re_τ

DNS setup

Flow case	Line style	Re_c	Re_τ	N_x	N_y	N_z	Δx^+	Δz^+	Tu_τ/h
C1	Dashed	3000	171	1280	192	896	7.55	4.80	113.9
C2	Dash-dot	4800	260	2048	256	1280	7.18	5.10	72.2
C3	Dash-dot-dot	10133	507	4096	384	2560	7.00	4.99	74.9
C4	Solid	21333	986	8192	512	5120	6.80	4.84	54.1

- Computational box $L_x = 18\pi h$, $L_z = 6\pi h$

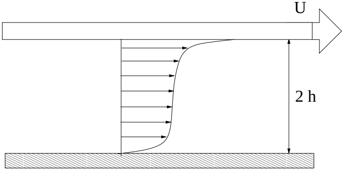

DNS of Couette flow

DNS at $Re_\tau = 1000$: contour lines of u'

low-speed and high-speed

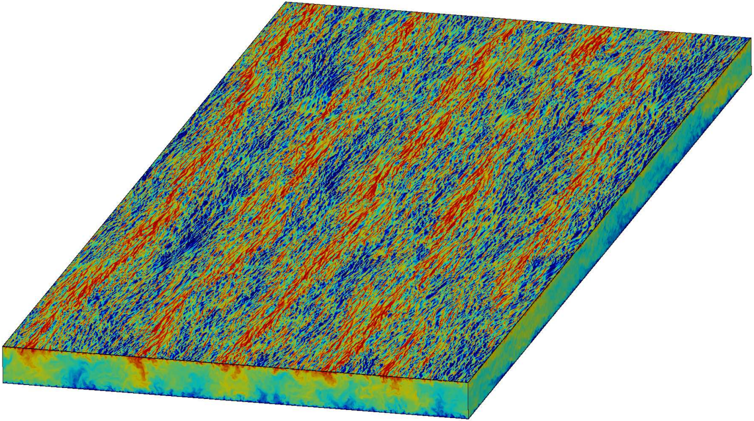

DNS of Couette flow

DNS at $Re_\tau = 1000$: contour lines of u'

low-speedand high-speed

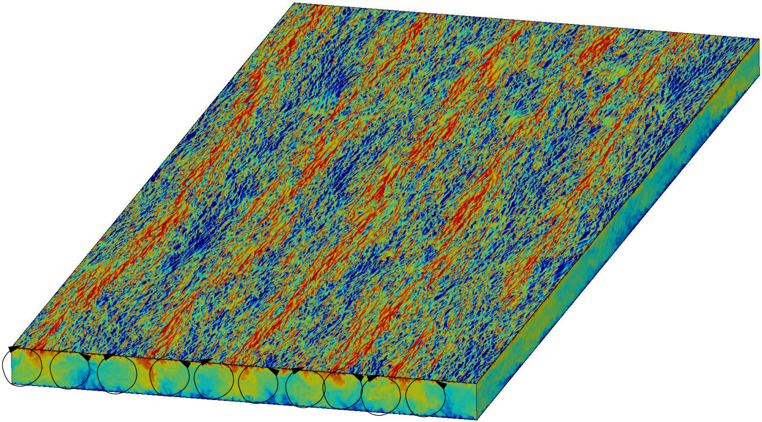

Mean velocity

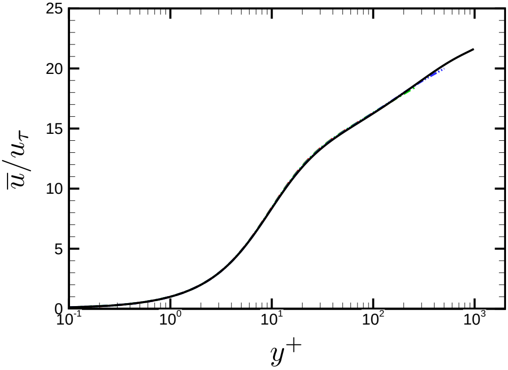

Mean velocity

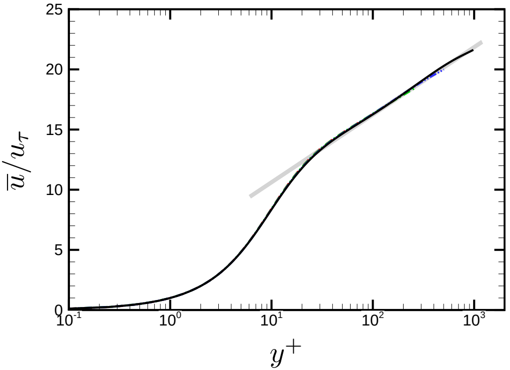

- Log-law fit $u^+ = 5.0 + \log y^+/0.41$

DNS of Couette flow

Diagnostic function $\Xi = y^+ \, \mathrm{d}\overline{u}^+ / \mathrm{d}y^+$

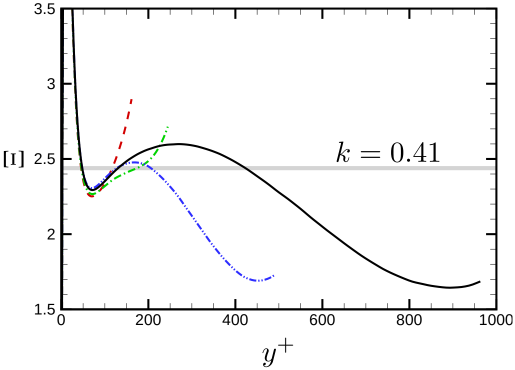

- No apparent tendency to log law !

Velocity variances

Horizontal components

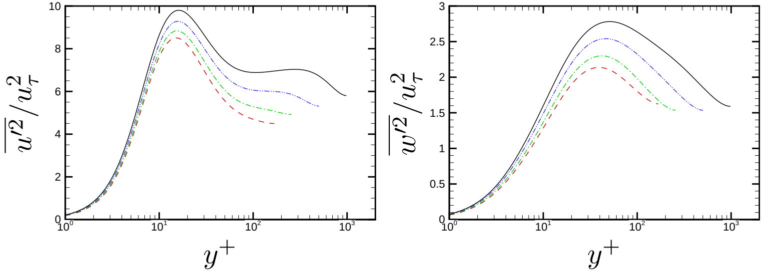

- Logarithmic decrease of w'
- Emergence of outer peak of u'

Reynolds stress peaks

Trend with Re_τ

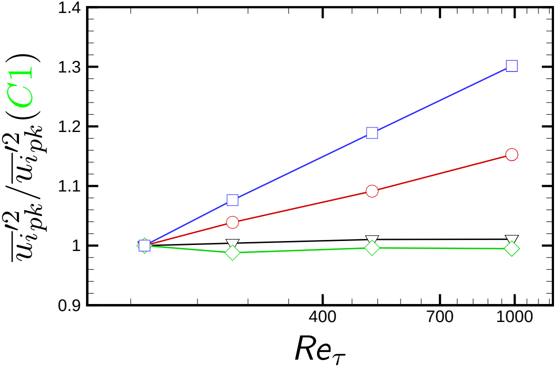

- Clear logarithmic growth of u and w
- No growth of v

Spectral densities (pre-multiplied)

Inner scaling

C1

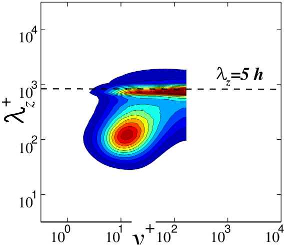

C2

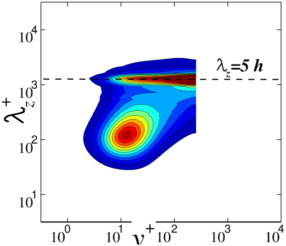

C3

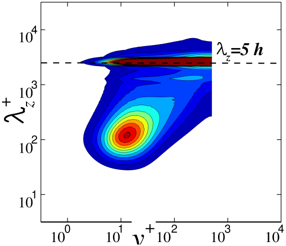

C4

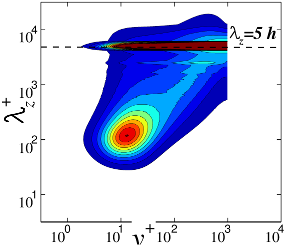

Production excess over dissipation

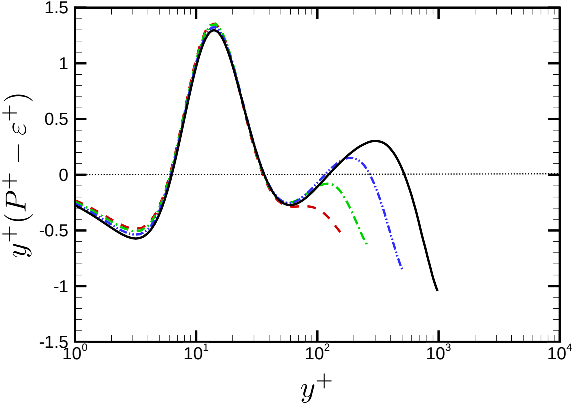

- Equilibrium hypothesis clearly violated at sufficiently high Re_τ

Coherent part of stresses

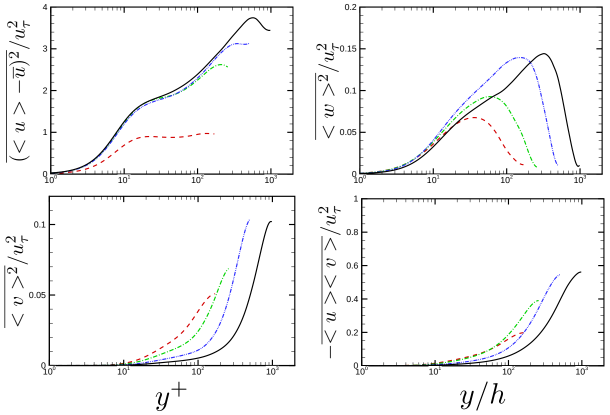

- Rollers responsible for significant fraction of Reynolds stresses

Computational set-up

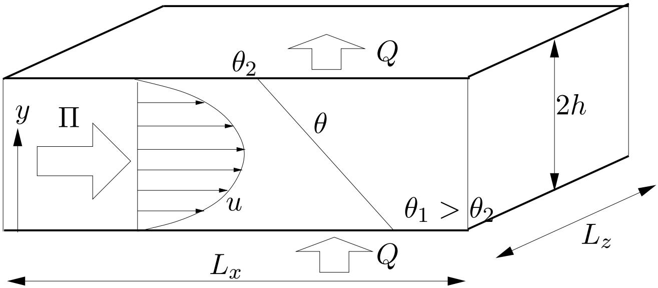

- Channel $\neq$ boundary layer
- Confined domain
- No rotation
- No roughness
- Imposed $\Delta\theta$

Streets of cumulus clouds

Flow cases

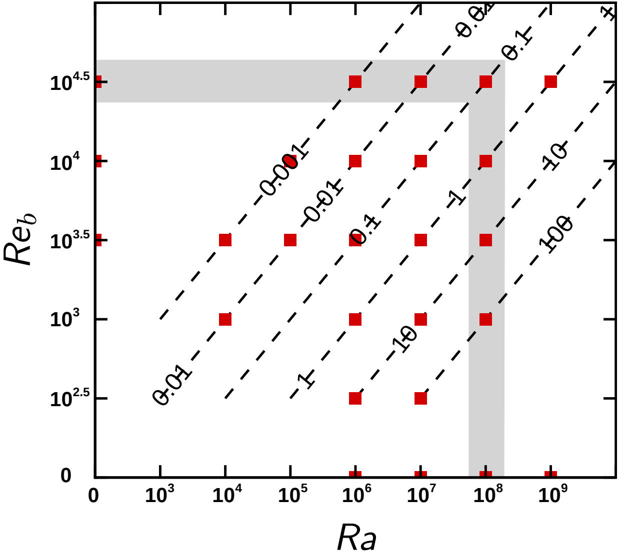

Re_b
$10^{4.5}$
10^4
$10^{3.5}$
10^3
$10^{2.5}$
0
0
10^3
10^4
10^5
10^6
10^7
10^8
10^9
Ra
-0.001
-0.01
0.1
-1
1
-10
10
100
0.01
0.1
0.01
1

Selection of computational mesh

- Grid selected so as to simultaneously satisfy
  - Spacing restriction for Rayleigh-Bénard convection (Shishkina et al. 2010)
  - Grid spacing restrictions for forced convection $\Delta x^+ \approx \Delta z^+ \approx 4.5$
  - For all simulations, $\Delta/\eta \lesssim 3$ throughout

- Box size is a sensitive issue (reminiscent of Couette flow) ...
- We eventually went for $L_x = 16h$, $L_z = 8h$

Flow cases

Flow case	Re_b	Ra	Ri_b	h/L	Re_τ	Nu	C_f	N_x	N_y	N_z
RUN_Ra9_Re0	0	10^9	∞	∞	0	63.172	NA	6144	768	3072
RUN_Ra9_Re4.5	31623	10^9	1	4.44264	946.41	60.255	7.16E-3	6144	768	3072
RUN_Ra8_Re0	0	10^8	∞	∞	0	30.644	NA	2560	512	1280
RUN_Ra8_Re3	1000	10^8	100	214.136	96.166	30.470	7.39E-2	2560	512	1280
RUN_Ra8_Re3.5	3162	10^8	10	30.0932	179.12	27.672	2.56E-2	2560	512	1280
RUN_Ra8_Re4	10000	10^8	1	3.67709	351.01	25.443	9.85E-3	2560	512	1280
RUN_Ra8_Re4.5	31623	10^8	0.1	0.44134	864.24	45.584	5.97E-3	2560	512	1280
RUN_Ra7_Re0	0	10^7	∞	∞	0	15.799	NA	1024	256	512
RUN_Ra7_Re2.5	316.2	10^7	100	167.716	38.690	15.541	1.20E-1	1024	256	512
RUN_Ra7_Re3	1000	10^7	10	24.4576	70.992	14.000	4.03E-2	1024	256	512
RUN_Ra7_Re3.5	3162	10^7	1	3.01888	134.98	11.880	1.46E-2	1024	256	512
RUN_Ra7_Re3.5_LA	3162	10^7	1	2.99729	136.12	12.094	1.48E-2	2048	256	1024
RUN_Ra7_Re3.5_SM	3162	10^7	1	2.85494	136.60	11.642	1.49E-2	512	256	256
RUN_Ra7_Re3.5_NA	3162	10^7	1	2.50569	142.59	11.622	1.62E-2	256	256	128
RUN_Ra7_Re4	10000	10^7	0.1	0.37257	307.01	17.250	7.54E-3	1024	256	512
RUN_Ra7_Re4.5	31623	10^7	0.01	0.04243	823.19	37.871	5.42E-3	2560	512	1280
RUN_Ra6_Re0	0	10^6	∞	∞	0	8.2884	NA	512	192	256
RUN_Ra6_Re2	100	10^6	100	114.745	16.436	8.1528	2.16E-1	512	192	256
RUN_Ra6_Re2.5	316.2	10^6	10	16.0776	30.527	7.3180	7.45E-2	512	192	256
RUN_Ra6_Re3	1000	10^6	1	1.94472	58.894	6.3560	2.77E-2	512	192	256
RUN_Ra6_Re3.5	3162	10^6	0.1	0.29783	112.47	6.7801	1.02E-2	512	192	256
RUN_Ra6_Re4	10000	10^6	0.01	0.02906	298.92	12.419	7.15E-3	1024	256	512
RUN_Ra6_Re4.5	31623	10^6	0.001	0.00349	817.63	30.508	5.35E-3	2560	512	1280
RUN_Ra5_Re3.5	3162	10^5	0.01	0.02262	108.48	4.6190	9.41E-3	512	192	256
RUN_Ra5_Re4	10000	10^5	0.001	0.00284	297.86	12.013	7.10E-3	1024	256	512
RUN_Ra4_Re3	1000	10^4	0.01	0.01508	45.731	2.3073	1.67E-2	512	192	256
RUN_Ra4_Re3.5	3162	10^4	0.001	0.00225	107.22	4.4345	9.19E-3	512	192	256
RUN_Ra0_Re3.5	3162	0	0	0	106.78	4.4836	9.12E-3	512	192	256
RUN_Ra0_Re4	10000	0	0	0	297.78	12.009	7.09E-3	1024	256	512
RUN_Ra0_Re4.5	31623	0	0	0	815.60	29.757	5.32E-3	2560	512	1280

Flow cases

DNS at $Ri = 1$: contour lines of θ'

cold and hot

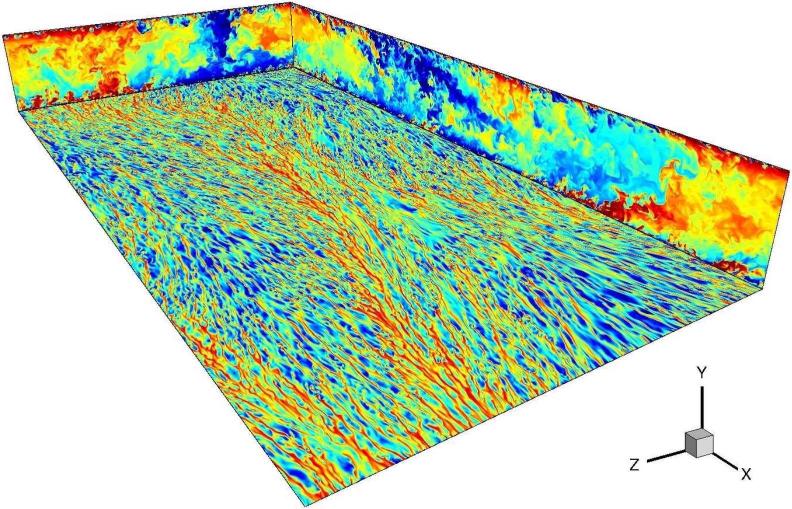

Spectra

Channel centerplane

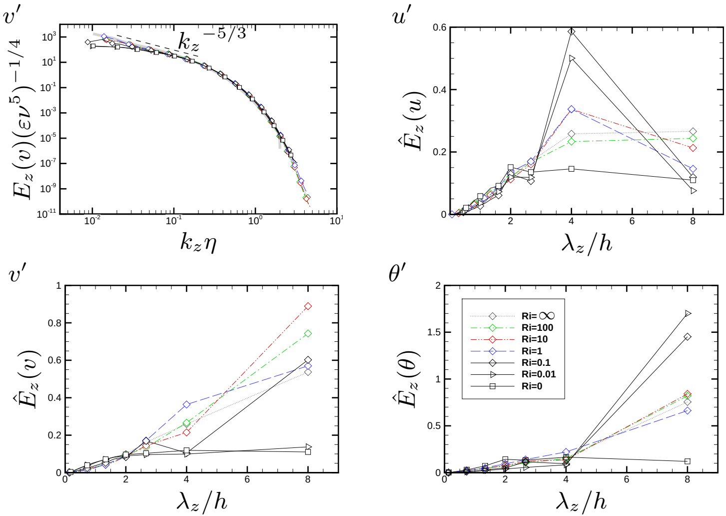

$$\lambda_v = \lambda_w = 2\lambda_u$$

Near-wall plane ($y = y_P$)

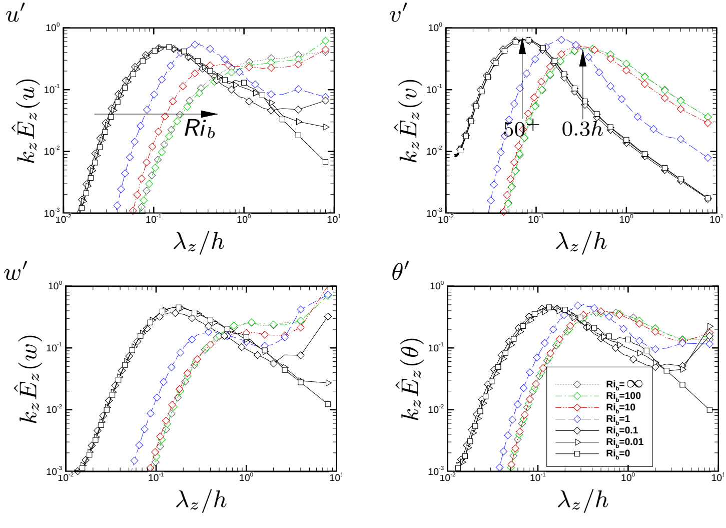

Free convection ($\mathrm{Ri}_b \to \infty$)

Expectations

- Prandtl (32):
  - the typical vertical velocity scale of buoyant plumes is $v_P = (\beta g Q y)^{1/3}$
  - the associated temperature scale is $\theta_P = Q^{2/3}(\beta g y)^{-1/3}$
  - $\mathrm{Pr}_t \approx$ const.
- Consequences
  - Scaling of mean velocity and temperature

$$\frac{\overline{\theta}(y) - \theta_0}{\theta_\tau} = 3B_\theta \left[(y/L)^{-1/3} - (y_0/L)^{-1/3} \right[$$

$$\frac{\overline{u}(y) - u_0}{u_\tau} = -3B_u \left[(y/L)^{-1/3} - (y_0/L)^{-1/3} \right]$$

  - Velocity fluctuations to scale as $\overline{v'^2}/u_\tau^2 \sim (y/L)^{2/3}$
  - Temperature fluctuations to scale as $\overline{\theta'^2}/\theta_\tau^2 \sim (y/L)^{-2/3}$

Free convection: power-law diagnostics

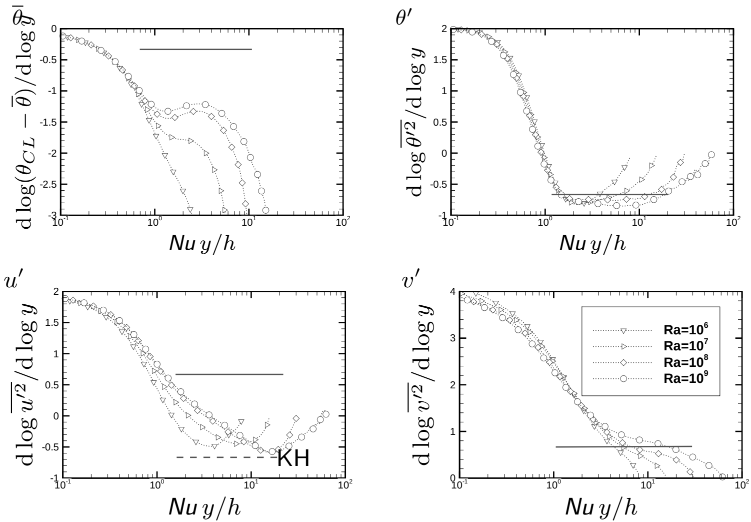

Kader & Yaglom 90: u' should depend on h-sized eddies $\sim (y/L)^{-2/3}$

Forced convection

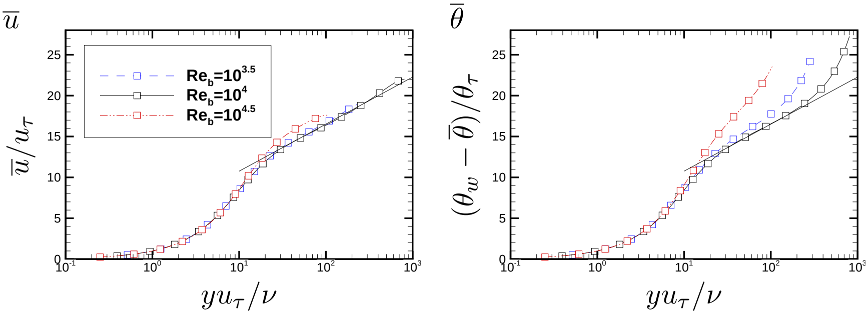

$$k \approx k_\theta \approx 0.4$$

Mean profiles

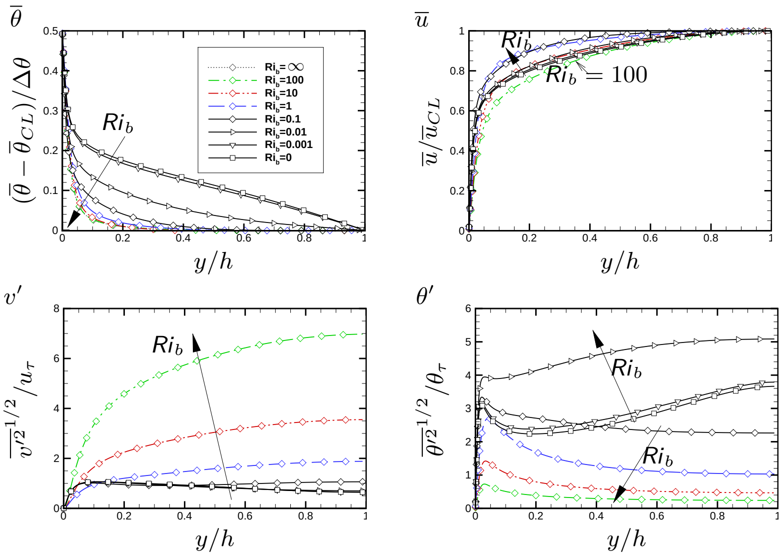

Fluxes and correlations

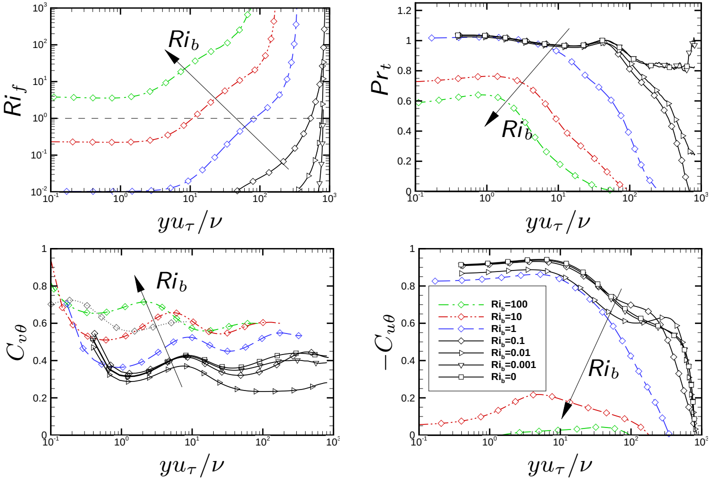

$$Ri_f = \frac{-\beta g \overline{v'\theta'}}{\overline{u'v'} \mathrm{d}\overline{u}/\mathrm{d}y}, \quad Pr_t = \frac{\nu_t}{\alpha_t} = \frac{\overline{u'v'}}{\overline{v'\theta'}} \frac{\mathrm{d}\overline{\theta}/\mathrm{d}y}{\mathrm{d}\overline{u}/\mathrm{d}y}$$

Monin-Obukhov similarity

- Obukhov 46, Monin & Obukhov 54: single length scale encapsulating effect of shear and buoyancy

$$L = \frac{u_\tau^3}{Q\beta g}$$

- Flow fully characterized by u_τ, L
- Constancy of total stress and total heat flux

$$-\overline{u'v'} \approx \tau_w, \quad -\overline{v'\theta'} \approx Q$$

- Universal representation

$$\frac{y}{\theta_\tau}\frac{\mathrm{d}\overline{\theta}}{\mathrm{d}y} = \varphi_h\left(\frac{y}{L}\right), \quad \frac{y}{u_\tau}\frac{\mathrm{d}\overline{u}}{\mathrm{d}y} = \varphi_m\left(\frac{y}{L}\right)$$

$$\frac{\overline{u_i'^2}^{1/2}}{u_\tau} = \varphi_i\left(\frac{y}{L}\right), \frac{\overline{\theta'^2}^{1/2}}{\theta_\tau} = \varphi_\theta\left(\frac{y}{L}\right), \quad \frac{-\overline{u'\theta'}}{Q} = \varphi_{u\theta}\left(\frac{y}{L}\right)$$

- Asymptotic behavior discussed by Kader & Yaglom 90

Parametrizations

- Unstable stratification: Businger 71, Dyer 74

$$\varphi_h = \frac{1}{k_\theta}\,(1+\gamma_h y/L)^{\alpha_h}\,, \quad \varphi_m = \frac{1}{k}\,(1+\gamma_m y/L)^{\alpha_m}\,,$$

- Typical choice (Paulson 70): $k = k_\theta = 0.35$, $\gamma_m = \gamma_h = 16$, $\alpha_h = -1/2$, $\alpha_m = -1/4$

Quantity	k_{DNS}	γ_{DNS}	α_{DNS}	α_{KY}	α_{BDP}
φ_h	0.375	5.67	−0.538	-1/3	-1/2
φ_m	0.399	14.6	−0.145	-1/3	-1/4
φ_1	0.498	0.830	0.361	1/3	/
φ_2	1.03	0.638	0.452	1/3	1/3
φ_θ	0.318	4.08	−0.420	-1/3	/
$\varphi_{u\theta}$	0.214	6.70	−0.690	-2/3	/

KY $\rightsquigarrow$ Kader & Yaglom 90, BDP $\rightsquigarrow$ Businger-Dyer-Panofsky

- Account for deviations from alleged free-convection scaling
- Widely used as wall models for LES of atmospheric BL (e.g. Khanna & Brasseur 97, 98)

DNS data

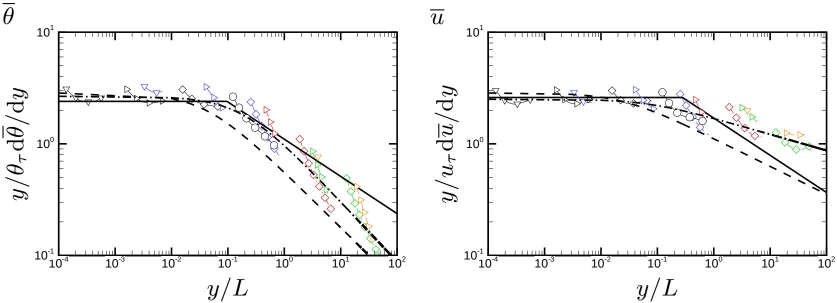

Solid: KY, Dashed: BDP; Chained: DNS fit

DNS data

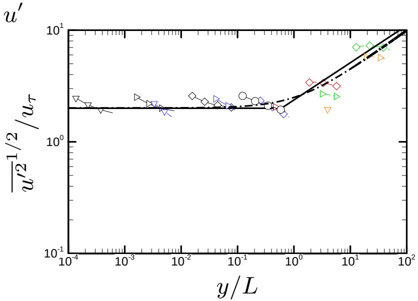

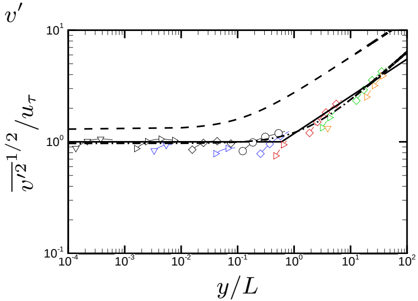

Solid: KY, Dashed: BDP; Chained: DNS fit

Monin-Obukhov similarity

DNS data

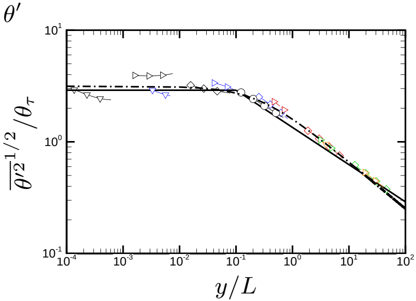

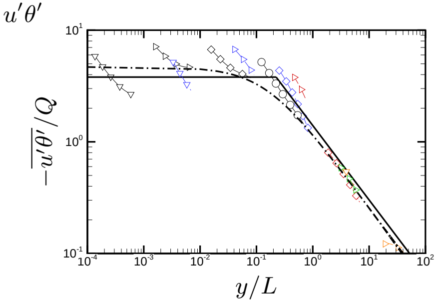

Solid: KY, Dashed: BDP; Chained: DNS fit

Summary

- DNS of canonical flows starting to approach Re_τ typical of 'asymptotic' wall turbulence
- Near log layer found for mean velocity
- Significant flow-dependent deviations: $Re_\tau \to \infty$ limit unclear
- Logarithmic growth of velocity variances confirmed: unbounded growth in wall units?
- Rollers form in wide variety of flow conditions ($0.01 \leq Ri_b \leq 100$)
- Aspect ratio 2 at least
- Strong modulation of near-wall region
- Prandtl scaling for natural convection does not show up
- Monin-Obukhov scaling applies to bulk flow, but not to individual profiles
- Significant deviations in light-wind regime
- DNS data available at
  `http://newton.dma.uniroma1.it/channel/`
  `http://newton.dma.uniroma1.it/couette/`
  `http://newton.dma.uniroma1.it/scalars/`